Stabilization of the propagation of spatial solitons

Matthew S. Bigelow, Q-Han Park,* and Robert W. Boyd†
Institute of Optics, University of Rochester, Rochester, New York 14627

(Received 12 March 2002; revised manuscript received 26 August 2002; published 30 October 2002)

We investigate a class of vector ring spatial solitons that carry no net angular momentum. Specifically, we show analytically and numerically that the dominant low-frequency perturbations that typically disrupt ring solitons are suppressed for these solitons. By comparing our analytical and numerical results, we show that our simple analysis gives good qualitative predictions on the regions of stability for these beams.

DOI: 10.1103/PhysRevE.66.046631 PACS number(s): 42.65.Tg

Optical spatial solitons (self-trapped light filaments) [1] hold great promise for many applications in modern optical technology [2]. However, it is well established that self-trapped beams (that is, $(2+1)$-dimensional waves) are unstable in a homogeneous Kerr medium [3]. Several techniques have been proposed and implemented for increasing the stability of spatial solitons, including the use of saturable nonlinear materials [4], geometries with restricted dimensionality [5], nonparaxial beams [6], and multicomponent (vector) solitons [7,8]. The components of a vector soliton can be orthogonal polarizations [9,10], fundamental and second harmonic components [11], or any two mutually incoherent beams [12]. The stability of spatial vector solitons has been the subject of active investigation over the past several years [13,14]. The stability of ring-shaped vector solitons was shown in the second harmonic generation process [15] while ring-shaped scalar solitons can be made stable in quintic nonlinear media [16–18]. But in general, the existence and stability of ring-shaped vector solitons remains an open question.

There has also been considerable interest in the formation of higher-order spatial solitons [19], that is, solitons possessing complex transverse structure leading to radial and/or azimuthal nodes of the field distribution. These highly structured, higher-order solitons possess considerable promise for applications because of their increased information content and power handling capabilities. The simplest nontrivial case of a higher-order soliton is the fundamental spinning soliton—the (scalar) ring-shaped beam described by Kruglov *et al.* [20] and Firth and Skryabin [21]. These authors point out that the dominant source of instability of such beams is the growth of azimuthal perturbations, and relate the origin of this instability to the (orbital) angular momentum [22] that is necessarily carried by such beams.

In this paper, we consider a class of vector ring solitons that possesses greatly improved stability. In contrast to a scalar ring soliton that carries a definite nonzero-angular momentum, each componant of a vector ring soliton can be made to possess equal and opposite angular momentum to produce a beam with no net angular momentum. We show that vector ring solitons that carry zero total angular momentum are more stable than the scalar ring soliton by performing both analytical and numerical studies of these vector ring solitons. Using a simplified analysis, we show that these zero-angular-momentum vector ring solitons are more resilient against the dominant, low-spatial frequency, azimuthal perturbations. In addition, we find that these beams possess an additional region of instability for a certain finite range of pertrubation frequencies (see Fig. 2 below). However, these instabilities can be suppressed by using beams that carry high power. These analytic predictions are in good agreement with numerical results that are also presented in this paper.

We assume that the vector soliton is comprised of two components of the form $E_1(r,\phi,z,t)=\psi_1(r,\phi,z)e^{i(kz-\omega t)}$ $+\text{c.c.}$ and $E_2(r,\phi,z,t)=\psi_2(r,\phi,z)e^{i(kz-\omega t)}+\text{c.c.}$ We take the equation that describes the propagation of this field as

$$-i\frac{\partial\psi_{1,2}}{\partial z}=\frac{1}{2k}\nabla_\perp^2\psi_{1,2}+F(|\psi_1|^2+|\psi_2|^2)\psi_{1,2}, \qquad (1)$$

where $\nabla_\perp^2$ is the transverse Laplacian, and $F(|\psi_1|^2+|\psi_2|^2)$ is a function of the total optical intensity. For a Kerr nonlinearity, this equation reduces to the Manakov equation by taking

$$F(|\psi_1|^2+|\psi_2|^2)=\gamma(|\psi_1|^2+|\psi_2|^2), \qquad (2)$$

where the parameter γ is related to the third-order nonlinear susceptibility by $\gamma=(6\pi\omega/n_0c)\chi^{(3)}$. For a saturable nonlinear optical medium, we model the nonlinear response as

$$F(|\psi_1|^2+|\psi_2|^2)=\frac{\gamma(|\psi_1|^2+|\psi_2|^2)}{1+\eta(|\psi_1|^2+|\psi_2|^2)}, \qquad (3)$$

where η is inversely proportional to the saturation intensity.

In this paper, we consider a class of solutions to Eq. (1) having the form

$$\psi_1(r,\phi,z)=\frac{1}{\sqrt{2}}R(r)e^{i\kappa z}e^{im\phi}, \qquad (4a)$$

$$\psi_2(r,\phi,z)=\frac{1}{\sqrt{2}}R(r)e^{i\kappa z}e^{\pm im\phi}. \qquad (4b)$$

*Also at Department of Physics, Korea University, 136-701, Korea. Email address: qpark@korea.ac.kr
†Also at Department of Physics and Astronomy, University of Rochester, Rochester, NY 14627.

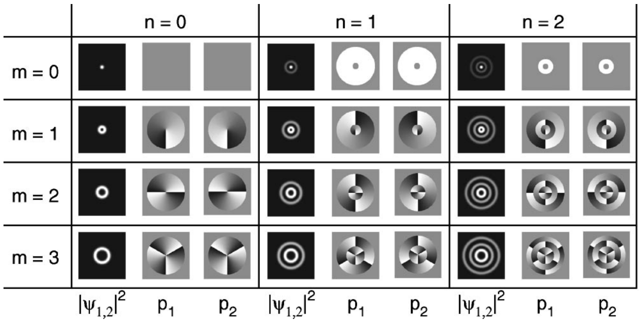

FIG. 1. The transverse intensity $|\psi_{1,2}|^2$ and phase (p_1 and p_2) distributions for each component of the vector ring soliton, for various values of the mode numbers *m* and *n*. For the $(m,-m)$ case, the phase of $\psi_{1,2}$ is shown as $p_{1,2}$. For the (m,m) case, the phase of both fields is given by p_1. The phase plots run from $-\pi$ (dark) to π (bright).

Here ψ_1 and ψ_2 represent the two components of the vector soliton, $R(r)$ represents their common radial dependence, κ is their common rate of nonlinear phase acquisition, and $\pm m$ two possible orbital angular momenta for the second component [23]. Note that κ increases monotonically with the power carried by the soliton. We will denote the cases of equal and opposite angular momenta by (m,m) and $(m,-m)$. Scalar solitons, for which (in our notation) either ψ_1 or ψ_2 vanishes, carry nonzero-angular momentum and are essentially equivalent to the (m,m) case after the symmetry rotation: $(\psi_1+\psi_2)/\sqrt{2}\rightarrow\psi_1$, $(\psi_1-\psi_2)/\sqrt{2}\rightarrow\psi_2$ under which Eq. (1) is invariant. In contrast, the total field carries zero-angular momentum in the $(m,-m)$ case. By introducing the trial solution (4) into the wave equation (1), we find that Eq. (4) is in fact a solution only if the radial function $R(r)$ obeys the equation

$$R''+\frac{1}{r}R'=\left(\frac{m^2}{r^2}+\beta^2\right)R-2kF(R^2)R, \tag{5}$$

where $\beta=\sqrt{2k\kappa}$ and, where R' and R'' are the first and second derivatives of *R* with respect to the radial coordinate *r*. When we apply the boundary condition for bright solitons that $R\rightarrow 0$ as $r\rightarrow\infty$, we find that, for each value of *m*, there is an infinite number of solutions $R(r)$. We label these solutions as $R_{nm}(r)$, where *n* represents the number of radial nodes in the solution. In Fig. 1 we show a representation of the intensity and phase of these solutions for different values of the mode numbers *n* and *m*.

We next address the stability of these solutions and demonstrate their enhanced robustness in the $(m,-m)$ case. We consider explicitly the case $n=0$, $m\geqslant 1$, although the method generalizes readily to higher-*n* solutions. This analysis is similar to one performed by Soto-Crespo *et al.* and others [24]. To perform the stability analysis, we consider perturbations of the form

$$\delta\psi_1=\frac{1}{\sqrt{2}}a_1(r,\phi,z)R(r)e^{i\kappa z}e^{im\phi}, \tag{6a}$$

$$\delta\psi_2=\frac{1}{\sqrt{2}}a_2(r,\phi,z)R(r)e^{i\kappa z}e^{\pm im\phi}. \tag{6b}$$

We introduce this form into the linearization of Eq. (1) to obtain

$$-i\frac{\partial a_1}{\partial z}=\frac{1}{2k}\left(\frac{\partial^2 a_1}{\partial r^2}+\frac{1}{r}\frac{\partial a_1}{\partial r}+\frac{1}{r^2}\frac{\partial^2 a_1}{\partial\phi^2}+\frac{2R'}{R}\frac{\partial a_1}{\partial r}+\frac{2im}{r^2}\frac{\partial a_1}{\partial\phi}\right)+\frac{1}{2}R^2F'(R^2)(a_1+a_1^*+a_2+a_2^*), \tag{7a}$$

$$-i\frac{\partial a_2}{\partial z}=\frac{1}{2k}\left(\frac{\partial^2 a_2}{\partial r^2}+\frac{1}{r}\frac{\partial a_2}{\partial r}+\frac{1}{r^2}\frac{\partial^2 a_2}{\partial\phi^2}+\frac{2R'}{R}\frac{\partial a_2}{\partial r}\pm\frac{2im}{r^2}\frac{\partial a_2}{\partial\phi}\right)+\frac{1}{2}R^2F'(R^2)(a_1+a_1^*+a_2+a_2^*), \tag{7b}$$

where F' denotes the derivative of F with respect to its argument.

Now we make the change of variables $a_1=\varepsilon_1+i\Delta_1$ and $a_2=\varepsilon_2+i\Delta_2$, and introduce the definitions $\varepsilon_\pm=\varepsilon_1\pm\varepsilon_2$, $\Delta_\pm=\Delta_1\pm\Delta_2$ to obtain

$$-\frac{\partial\varepsilon_\pm}{\partial z}=\frac{1}{2k}\left(\frac{\partial^2\Delta_\pm}{\partial r^2}+\frac{1}{r}\frac{\partial\Delta_\pm}{\partial r}+\frac{1}{r^2}\frac{\partial^2\Delta_\pm}{\partial\phi^2}+\frac{2R'}{R}\frac{\partial\Delta_\pm}{\partial r}+\frac{2m}{r^2}\frac{\partial E_\pm}{\partial\phi}\right), \tag{8a}$$

$$\frac{\partial\Delta_\pm}{\partial z}=\frac{1}{2k}\left(\frac{\partial^2\varepsilon_\pm}{\partial r^2}+\frac{1}{r}\frac{\partial\varepsilon_\pm}{\partial r}+\frac{1}{r^2}\frac{\partial^2\varepsilon_\pm}{\partial\phi^2}+\frac{2R'}{R}\frac{\partial\varepsilon_\pm}{\partial r}-\frac{2m}{r^2}\frac{\partial D_\pm}{\partial\phi}\right)+2R^2F'(R^2)M_\pm, \tag{8b}$$

where $M_+=\varepsilon_+$, $M_-=0$. We have $E_\pm=\varepsilon_\pm$, $D_\pm=\Delta_\pm$ for the (m,m) case and $E_\pm=\varepsilon_\mp$, $D_\pm=\Delta_\mp$ for the $(m,-m)$ case. In order to check stability under perturbations, we seek a solution with definite angular dependence of the form,

$$\varepsilon_\pm(z,r,\phi)=\varepsilon^\pm(r)\cos(\Lambda z+\Omega\phi), \tag{9a}$$

$$\Delta_\pm(z,r,\phi)=\Delta^\pm(r)\sin(\Lambda z+\Omega\phi), \tag{9b}$$

so that the linearized equation reduces to the eigenvalue problem with eigenvalue Λ,

$$\Lambda\varepsilon^\pm=\frac{1}{2k}\left(\frac{d^2\Delta^\pm}{dr^2}+\frac{1}{r}\frac{d\Delta^\pm}{dr}-\frac{\Omega^2}{r^2}\Delta^\pm+\frac{2R'}{R}\frac{d\Delta^\pm}{dr}-\frac{2m\Omega}{r^2}E^\pm\right), \tag{10a}$$

$$\Lambda\Delta^{\pm}=\frac{1}{2k}\left(\frac{d^2\varepsilon^{\pm}}{dr^2}+\frac{1}{r}\frac{d\varepsilon^{\pm}}{dr}-\frac{\Omega^2}{r^2}\varepsilon^{\pm}+\frac{2R'}{R}\frac{d\varepsilon^{\pm}}{dr}-\frac{2m\Omega}{r^2}D^{\pm}\right)+2R^2F'(R^2)M^{\pm}, \tag{10b}$$

where $E^{\pm}$, $D^{\pm}$, and $M^{\pm}$ are same as before except that the cosine and the sine factors are absent. In principle, this eigenvalue problem can be solved numerically to determine the eigenvalue Λ; if Λ possesses an imaginary part, the solution is unstable. However, in order to develop an analytic understanding of the eigenvalue problem, we make an approximation by assuming that the stability is governed dominantly by field fluctuations around the peak of the ring vector soliton, i.e., at $r=r_0$ where $R'(r_0)=0$. We construct Taylor expansions around $r=r_0$ for the quantities $\Delta^{\pm}(r)\simeq\Delta_0^{\pm}(r_0)+(r-r_0)\Delta_1^{\pm}(r_0)$, $\epsilon^{\pm}(r)\simeq\epsilon_0^{\pm}(r_0)+(r-r_0)\epsilon_1^{\pm}(r_0)$, and $1/r\simeq 1/r_0-(r-r_0)/r_0^2$ where $\epsilon_1^{\pm}(r_0)\equiv d\epsilon^{\pm}(r)/dr|_{r_0}$ and $\Delta_1^{\pm}(r_0)\equiv d\Delta^{\pm}(r)/dr|_{r_0}$. With this expansion, we approximate the eigenvalue equations (10) by keeping terms up to first order in $\delta r=r-r_0$. To begin with, we will look at the zeroth-order part of our approximation. These assumptions are strictly valid for the case of a very thin ring, but even for a broad ring case they provide a good qualitative description of stability and agree quite well with numerical results we present later in this paper. With these assumptions, the eigenvalue equation reduces to

$$\Lambda\varepsilon_0^{\pm}=-\frac{\Omega^2}{2kr_0^2}\Delta_0^{\pm}-\frac{m\Omega}{kr_0^2}E_0^{\pm}, \tag{11a}$$

$$\Lambda\Delta_0^{\pm}=-\frac{\Omega^2}{2kr_0^2}\varepsilon_0^{\pm}-\frac{m\Omega}{kr_0^2}D_0^{\pm}+2R_0^2F'(R_0^2)M_0^{\pm}, \tag{11b}$$

where the subscript $_0$ signifies evaluation of quantities at $r=r_0$. Now we consider the (m,m) and $(m,-m)$ cases separately. The eigenvalue equation for the (m,m) case can be compactly written in a matrix form as

$$L\Psi=0, \tag{12}$$

where the 4×4 matrix L and the vector Ψ are given by

$$\Psi^T=(\varepsilon_0^+,\Delta_0^+,\varepsilon_0^-,\Delta_0^-) \tag{13a}$$

$$L=\begin{pmatrix}\Lambda+2\xi m\Omega & \xi\Omega^2 & 0 & 0\\ -2R_0^2F'(R_0^2)+\xi\Omega^2 & \Lambda+2\xi m\Omega & 0 & 0\\ 0 & 0 & \Lambda+2\xi m\Omega & \xi\Omega^2\\ 0 & 0 & \xi\Omega^2 & \Lambda+2\xi m\Omega\end{pmatrix}, \tag{13b}$$

where $\xi=1/2kr_0^2$. The characteristic equation,

$$\det L=\{(\Lambda+2\xi m\Omega)^2-\xi\Omega^2[\xi\Omega^2-2R_0^2F'(R_0^2)]\}\times[(\Lambda+2\xi m\Omega)^2-(\xi\Omega^2)^2]=0, \tag{14}$$

immediately shows that complex Λ arises only if

$$\xi\Omega^2<2R_0^2F'(R_0^2). \tag{15}$$

Thus, the (m,m)-ring vector soliton becomes unstable when the angular frequency of azimuthal perturbation is below the critical value $\Omega<\Omega_c=2r_0R_0\sqrt{kF'(R_0^2)}$.

In the $(m,-m)$ case, the matrix L becomes

$$L=\begin{pmatrix}\Lambda & \xi\Omega^2 & 2\xi m\Omega & 0\\ -2R_0^2F'(R_0^2)+\xi\Omega^2 & \Lambda & 0 & 2\xi m\Omega\\ 2\xi m\Omega & 0 & \Lambda & \xi\Omega^2\\ 0 & 2\xi m\Omega & \xi\Omega^2 & \Lambda\end{pmatrix}. \tag{16}$$

The characteristic equation now has the form

$$\det L=-\Lambda^4+A\Lambda^2-B=0,$$

$$A=8m^2\Omega^2\xi^2+2\Omega^4\xi^2-2R_0^2F'(R_0^2)\Omega^2\xi,$$

$$B=\xi^3\Omega^4(\Omega^2-4m^2)(\Omega^2\xi-4\xi m^2-2R_0^2F'(R_0^2)). \tag{17}$$

In order for Λ to be real, Λ^2 has to be non-negative real. This condition can be met when A, B and the discriminant A^2-4B are all non-negative. Thus, the $(m,-m)$-ring vector soliton becomes stable when the frequency Ω lies in the domain satisfying the following three restrictions;

$$\text{(i)}\quad \Omega^2\geqslant 2kr_0^2R_0^2F'(R_0^2)-4m^2, \tag{18a}$$

$$\text{(ii)}\quad \Omega^2\leqslant 4m^2 \ \text{ or } \ \Omega^2\geqslant 4m^2+4kr_0^2R_0^2F'(R_0^2), \tag{18b}$$

$$\text{(iii)}\quad \Omega^2\geqslant 2kr_0^2R_0^2F'(R_0^2)-\frac{[kr_0^2R_0^2F'(R_0^2)]^2}{4m^2}. \tag{18c}$$

In Fig. 2 we summarize the expressions from Eqs. (15) and (18) and show the regions of stability and instability for

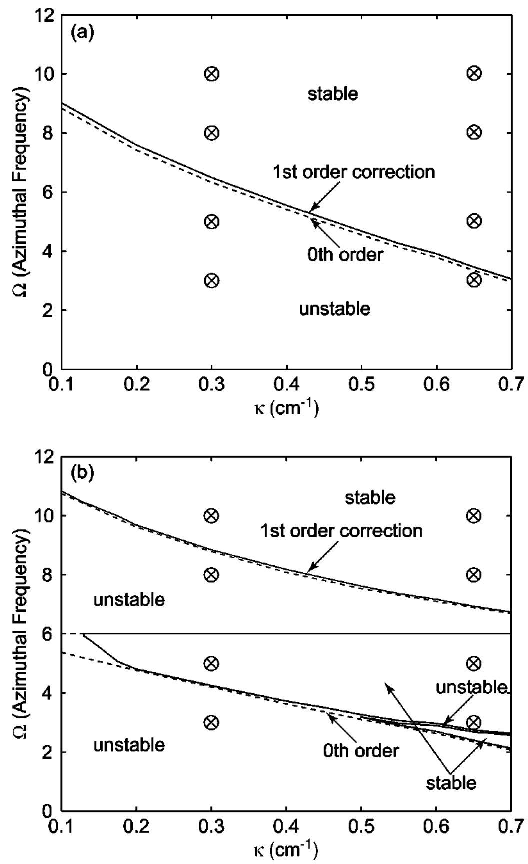

FIG. 2. The regions of stability and instability of azimuthal perturbations to exponential growth for the R_{03} mode. The dashed line corresponds to the zeroth-order terms in the Taylor expansion and the solid line is the first-order correction. (a) The regions of stability for the (m,m) case. (b) The regions of stability for the $(m,-m)$ case. Beams with azimuthal perturbation frequencies indicated by points on the graphs are shown before and after propagating through a saturable nonlinear medium in Figs. 3 and 4.

different azimuthal frequencies as a function of κ (dashed line). For the sake of argument, we have assumed the material to be a saturable nonlinear medium, but analogous diagrams can be drawn for a Kerr nonlinearity. To improve the approximations made earlier, we repeated the above analysis including terms up to first order in the Taylor expansion. When we do this L becomes a 8×8 matrix, and the corresponding regions of stability are slightly modified (solid line in Fig. 2).

We can make several observations about Fig. 2. First, we note that the thin ring approximation breaks down when κ is small in the $(m,-m)$ case. This is not surprising since the ring broadens out considerably at these lower values. Also, the large regions where the beams are nearly stable for large values of κ are comparable to the results of Mihalache *et al.* who report similar behavior [25,26]. However, they considered only spinning solitons, that is, the (m,m) case in our notation. Finally, the most significant result between the (m,m) case and the $(m,-m)$ case is that the $(m,-m)$ beam has a smaller region of instability at lower frequencies. By creating a beam that has a zero net angular momentum, we can suppress the growth of lower angular frequency perturbations that tend to dominate. In addition we observe in the numerical work described that perturbations in both the lower and middle instability regions do not grow as fast in the $(m,-m)$ case as they do in the lower region of the (m,m) case.

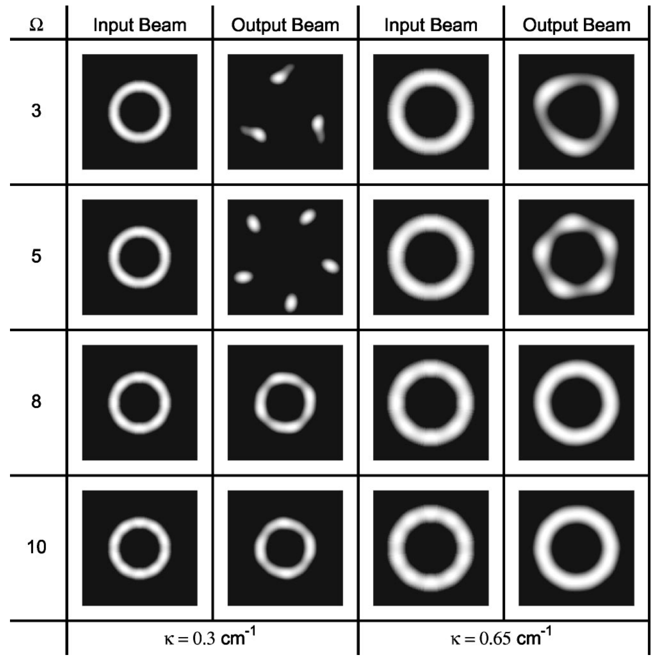

FIG. 3. The input and output beams with four different azimuthal frequency perturbations for the (m,m) case vector soliton $(m=3)$.

To show this, we performed numerical integrations of the propagation equation (1) using the split-step method [27] to

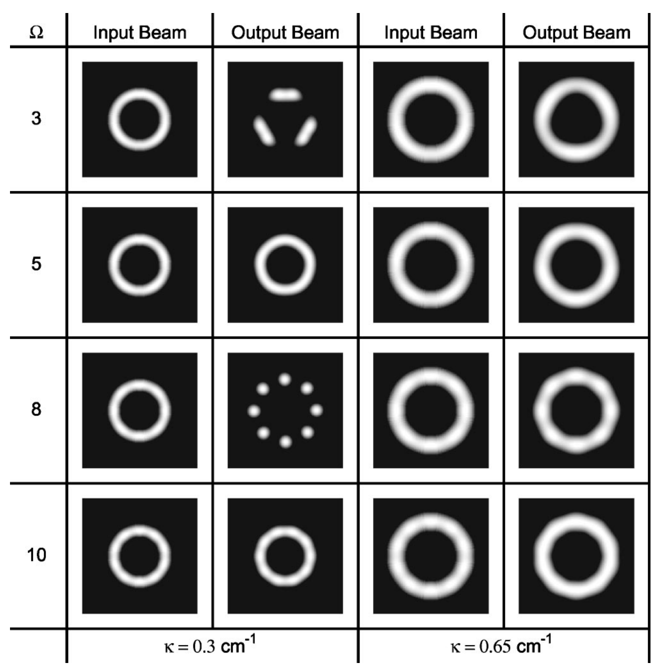

FIG. 4. The input and output beams with the same azimuthal frequency perturbations for the $(m,-m)$ case vector soliton $(m=3)$.

explore the stability of the vector ring solitons in the different regions. We show in Figs. 3 and 4 the output of a vector soliton beam with small (less than 10% amplitude) complex azimuthal perturbations propagating in a saturable nonlinear medium for two different values of κ. In performing these calculations we assume the parameters $z=50$ cm, $\gamma=1.95\times10^{-6}$ cm^2/erg, $\eta=2.49\times10^{-6}$ cm^3/erg, and $k=1.28\times10^5$ cm^{-1}.

For the (m,m) case (Fig. 3) we can clearly see the beam breaking up and the individual filaments diverging from one another when the perturbation spatial frequency is $\Omega=3$ and 5 for $\kappa=0.3$ cm^{-1}. Beam rotation as a result of a net angular momentum can also be seen. For $\kappa=0.65$ cm^{-1}, the beam has improved stability at these frequencies as both Fig. 2(a) and Ref. [25] suggests. In contrast, for the value of $\kappa=0.3$ cm^{-1}, Fig. 4 shows that the perturbations to the $(m,-m)$ beam grow at frequencies $\Omega=3$ and $\Omega=8$ on either side of a region of stability at $\Omega=5$. This region of stability is predicted by our analytical theory shown in Fig. 2(b). When we increase the value of κ to 0.65 cm^{-1}, we see that the beam becomes essentially stable over all of these frequencies.

In conclusion, we have analyzed a class of vector ring solitons that possesses enhanced stability characteristics. These solitons have zero net angular momentum, and consequently they possess a greater degree of stability than do standard ring solitons. To show this we have conducted a simple analytical analysis of the system's eigenvalues to find the frequency regions where the rings are unstable, and have shown through numerical simulations that these regions exist. Therefore, the simplifying assumption that the rings are thin which we made while performing the analytical analysis is a good way to predict qualitatively the regions of stability for vector ring solitons. In particular, we have found that low-frequency azimuthal perturbations of the soliton amplitude are suppressed. These results suggest that vector ring solitons with zero net angular momentum may have important applications in high-power laser systems. We also believe these vector solitons can be experimentally observed in a variety of material systems.

We thank J. Heebner for helpful discussions. This work was supported by AFOSR Grant No. F49620-00-1-0061, ONR Grant No. N00014-99-1-0539, ARO Grant No. DAAD19-01-1-0623, the U.S. Department of Energy Office of Inertial Confinement Fusion under Cooperative Agreement No. DE-FC03-92SF19460, and the University of Rochester. The support of DOE does not constitute an endorsement by DOE of the views expressed in this article. Q.P. is supported by Grant No. KRF-2001-015-DS0016.

[1] R.Y. Chiao, E. Garmire, and C.H. Townes, Phys. Rev. Lett. **13**, 479 (1964).
[2] G.I. Stegeman and M. Segev, Science **286**, 1518 (1999).
[3] See, e.g., L. Bergé, Phys. Rep. **303**, 260 (1998).
[4] Y. Chen, Opt. Lett. **16**, 4 (1991); M. Karlsson, Phys. Rev. A **46**, 2726 (1992); D.N. Christodoulides, T.H. Coskun, and R.I. Joseph, Opt. Lett. **22**, 1080 (1997).
[5] A. Barthelemy, S. Maneuf, and C. Froehly, Opt. Commun. **55**, 201 (1985); J.S. Aitchison *et al.*, J. Opt. Soc. Am. B **8**, 1290 (1991).
[6] N.N. Rozanov, N.V. Vysotina, and A.G. Vladimirov, JETP **91**, 1130 (2000).
[7] Z.H. Musslimani, M. Segev, D.N. Christodoulides, and M. Soljacic, Phys. Rev. Lett. **84**, 1164 (2000).
[8] J.J. García-Ripoll, V.M. Pérez-García, E.A. Ostrovskaya, and Y.S. Kivshar, Phys. Rev. Lett. **85**, 82 (2000).
[9] S.V. Manakov, Zh. Eksp. Teor. Fiz. **65**, 505 (1973) [Sov. Phys. JETP **38**, 248 (1974)].
[10] J.U. Kang, G.I. Stegeman, J.S. Aitchison, and N. Akhmediev, Phys. Rev. Lett. **76**, 3699 (1996).
[11] X. Liu, L.J. Qian, and F.W. Wise, Phys. Rev. Lett. **82**, 4631 (1999).
[12] M. Mitchell, Z. Chen, M.-F. Shih, and M. Segev, Phys. Rev. Lett. **77**, 490 (1996).
[13] D.E. Pelinovsky and Y.S. Kivshar, Phys. Rev. E **62**, 8668 (2000).
[14] E.A. Ostrovskaya, Y.S. Kivshar, D.V. Skryabin, and W.J. Firth, Phys. Rev. Lett. **83**, 296 (1999).
[15] I. Towers, A.V. Buryak, R.A. Sammut, and B.A. Malomed, Phys. Rev. E **63**, 055601(R) (2001).
[16] M. Quiroga-Teixeiro and H. Michinel, J. Opt. Soc. Am. B **14**, 2004 (1997).
[17] I. Towers *et al.*, Phys. Lett. A **288**, 292 (2001).
[18] R.L. Pego and H.A. Warchall, J. Nonlinear Sci. **12**, 347 (2002).
[19] H.A. Haus, Appl. Phys. Lett. **8**, 128 (1966).
[20] V.I. Kruglov, Y.A. Logvin, and V.M. Volkov, J. Mod. Opt. **39**, 2277 (1992).
[21] W.J. Firth and D.V. Skryabin, Phys. Rev. Lett. **79**, 2450 (1997).
[22] L. Allen, M.W. Beijersbergen, R.J.C. Spreeuw, and J.P. Woerdman, Phys. Rev. A **45**, 8185 (1992).
[23] In general, angular momenta for two components can be any two integers m_1,m_2. This requires distinct propagation constants κ_1,κ_2 and radial functions $R_1(r),R_2(r)$. The simple case of common radial function $R_1(r)=R_2(r)$ is possible only when $m_1=m$ and $m_2=\pm m$.
[24] J.M. Soto-Crespo, D.R. Heatley, E.M. Wright, and N.N. Akhmediev, Phys. Rev. A **44**, 636 (1991).
[25] B.A. Malomed, L.C. Crasovan, and D. Mihalache, Physica D **161**, 187 (2002).
[26] D. Mihalache *et al.*, Phys. Rev. Lett. **88**, 073902 (2002).
[27] See, for instance, G. P. Agrawal, *Nonlinear Fiber Optics*, Second Edition (Academic Press, San Diego, 1995), Sec. 2.4.1.